Jurnal Teknokes
Homepage: teknokes.org; Vol. 19, No. 1, pp. 034-047, March 2026;
e-ISSN: 2407-8964
p-ISSN: 1907-7904

RESEARCH PAPER

OPEN ACCES

Comparative Analysis of Hybrid Wavelet Transformation and Filter Bank for Efficient Arrhythmia Detection in ECG Signals

Amalia Nurul Maulida[1], Annisa Humairani[1,2], Tito Waluyo Purboyo[1,2], and Dziban Naufal[1,2]

[1] School of Electrical Engineering, Telkom University, Bandung, Indonesia

[2] Center of Excellence for Biomedical and Healthcare Technology, Research Institute for Digital Health, Social and Wellness, Telkom University, Bandung, Indonesia

ABSTRACT

Cardiovascular disease (CVD) is still the leading cause of death worldwide, and arrhythmia is one of its most serious forms because it can trigger sudden cardiac arrest. Given the life-threatening nature of arrhythmias, reliable automated methods for arrhythmia detection are increasingly important in both clinical and remote monitoring settings. While the electrocardiogram (ECG) is the standard tool for arrhythmia detection, its accuracy is often reduced by noise and waveform distortion, which may lead to misclassification. To address this challenge, this study proposes an arrhythmia classification framework that integrates wavelet-based feature extraction with filter bank enhancement. ECG signals from the MIT-BIH Arrhythmia Database were preprocessed and segmented from two leads (MLII and V1), followed by wavelet decomposition using Daubechies (db6), Symlet (sym7), and Biorthogonal (bior4.4) families. Three complementary feature enhancement schemes, Discrete Cosine Transform (DCT), Complex Discrete Wavelet Transform (CDWT), and Orthogonal filter bank, were applied prior to classification with Support Vector Machine (SVM) and Random Forest (RF). The experimental results further highlight that the selection of wavelet, filter bank, and classifier combinations significantly influences arrhythmia detection performance. In particular, the pairing of the bior4.4 wavelet with the orthogonal filter bank and RF classifier achieved the highest accuracy of 94.76%, outperforming other setups, including CDWT-based schemes. This outcome suggests that the linear phase property of bior4.4 yields a more stable feature representation that aligns well with the ensemble mechanism of RF. These insights reinforce the importance of considering both the mathematical properties of wavelets and classifier design when developing ECG-based diagnostic systems. Future work will extend this approach to deep learning models and larger datasets to strengthen its clinical applicability.

PAPER HISTORY

Received January 17, 2026
Revised January 31, 2026
Accepted February 28, 2026
Published March 18, 2026

KEYWORDS

Arrythmia;
Electrocardiogram;
Wavelet transform;
Filter bank;

CONTACT:

aamalianm@student.telkomuniversity.ac.id
annisahumairani@telkomuniversity.ac.id
titowaluyo@telkomuniversity.ac.id
dziban@telkomuniversity.ac.id

I. INTRODUCTION

Cardiovascular disease continues to be a major cause of mortality both globally and in Indonesia. A recent analysis in the Global Burden of Cardiovascular Diseases and Risks confirms that CVDs remain the top cause of death worldwide [1]. In Indonesia, evidence from the 30 Years of Shifting in the Indonesian Cardiovascular Burden shows that stroke and ischemic heart disease remain the principal contributors to mortality [2]. Furthermore, a 2024 study on multimorbidity among adults with cardiovascular diseases highlights the growing healthcare and economic burden of CVDs in Indonesia [3].

Within this spectrum of diseases, arrhythmia occupies a crucial position. Arrhythmia is defined as an abnormal heart rhythm that beats too fast, too slow, or irregularly due to dysfunction in the heart's electrical conduction system [4][5]. Recent clinical evidence shows that atrial fibrillation and ventricular arrhythmia in particular, are closely associated with an increased risk of stroke, worsening heart failure, and sudden death, placing arrhythmia as one of the main determinants of poor clinical outcomes [6][7][8][9][10]. Electrocardiography (ECG) is currently considered the standard method for detecting arrhythmia because it can record the heart's

Corresponding author: Annisa Humairani, annisahumairani@telkomuniversity.ac.id, School of Electrical Engineering, Telkom University, Bandung, Jl. Telekomunikasi No. 1, Sukapura, Kecamatan Dayeuhkolot, Kab. Bandung, Jawa Barat 40257.
DOI: https://doi.org/10.35882/jteknokes.v19i1.154

e-ISSN: 2407-8964
p-ISSN: 1907-7904

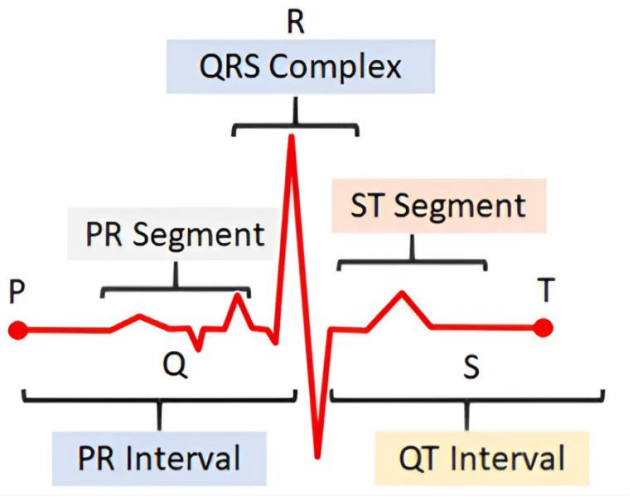

Fig. 1 Standard ECG waveform showing P wave, QRS complex, T wave, and key intervals (PR, ST, QT) [14].

electrical activity non-invasively and informatively [11]. However, the accuracy of ECG-based diagnosis is often compromised by noise and artifacts that contaminate the signal. Disturbances such as baseline wander from patient movement, electrode contact interference, or muscle activity can distort the P, QRS, and T waveforms. In addition, electrical interference entering through the electrodes may further degrade signal quality. As illustrated in Fig. 1, such distortions are particularly evident in ambulatory recordings and can mask critical wave components, thereby reducing the reliability of diagnosis and increasing the risk of misinterpretation and misdiagnosis [12][13].

Various approaches have been developed to denoise EKG signals and improve arrhythmia detection accuracy. One of them is Empirical Mode Decomposition (EMD), which is widely used in non-linear and non-stationary signals. Although effective, this method is highly dependent on the parameters used, so the decomposition results are not always stable [15]. Another approach is the Short-Time Fourier Transform (STFT), which represents signals in the time-frequency domain, but its window-size limitations make its resolution suboptimal, so some important information may be lost [16]. Another widely applied technique is the Hilbert–Huang Transform (HHT), which combines EMD with Hilbert spectral analysis to capture the instantaneous frequency of non-stationary signals. However, this method still suffers from mode mixing and boundary effects, which can reduce the clarity and reliability of the results [17]. Furthermore, Variational Mode Decomposition (VMD) has been proposed as a more adaptive decomposition method that iteratively decomposes a signal into a finite number of band-limited intrinsic mode functions (IMFs). While VMD generally overcomes the mode-mixing problem associated with EMD by solving a constrained variational optimization problem, it still requires the number of decomposition modes to be specified in advance, and its iterative optimization process renders it significantly more computationally expensive than EMD or STFT, making it less practical for real-time or large-scale ECG analysis [41]. Another commonly used technique is the Continuous Wavelet Transform (CWT), which offers excellent time-frequency localization through scalable, shift-invariant basis functions. Although CWT provides high resolution across both the time and frequency domains and has been applied to ECG feature extraction, it generates a highly redundant, large-scale coefficient matrix that increases memory consumption and computational load substantially, limiting its efficiency in multi-class arrhythmia classification tasks [42]. Additionally, deep learning approaches, particularly Convolutional Neural Networks (CNNs) and Long Short-Term Memory (LSTM) networks, have gained prominence in automated arrhythmia detection due to their ability to learn hierarchical representations directly from raw ECG data. While these methods can achieve state-of-the-art accuracy, they typically require large annotated training datasets, substantial computational resources (GPU acceleration), and long training times, which constrain their applicability in resource-limited or embedded clinical environments [43]. Thus, despite many methods, it remains difficult to find an approach that balances temporal resolution, spectral accuracy, and computational efficiency simultaneously.

This limitation then became the research gap that underpinned this study. Most previous studies focused on either a single decomposition method or deep learning-based approaches, which, although powerful, required substantial computational resources and large amounts of annotated data. Meanwhile, systematic exploration of the combination of wavelet decomposition with filter banks, which has the potential to produce lightweight but effective methods, is still relatively limited. This gap highlights the need for research to design strategies that can produce high-quality features, retain temporal and frequency information simultaneously, and remain computationally efficient.

To address these challenges, this study proposes a hybrid framework that integrates wavelet decomposition with three types of filter banks, namely DCT, CDWT, and orthogonal filter banks. The extracted features are then classified using two commonly used machine learning algorithms, namely SVM and RF. In addition, three wavelet families, namely db6, sym7, and bior4.4, are also systematically evaluated to take advantage of the multi-resolution properties of ECG signals and assess how different wavelet bases interact with filter banks in influencing classification results.

The main objective of this study is to assess how the selection of wavelet bases, filter bank design, and classification algorithms affect the accuracy of arrhythmia detection, and to identify combinations that deliver high performance and computational efficiency. By integrating various decomposition and filtering strategies into a single comparative framework, this study not only seeks to improve classification results but also emphasizes the importance of compatibility between signal representation techniques and classification models. Thus, this research

Corresponding author: Annisa Humairani, annisahumairani@telkomuniversity.ac.id, School of Electrical Engineering, Telkom University, Bandung, Jl. Telekomunikasi No. 1, Sukapura, Kecamatan Dayeuhkolot, Kab. Bandung, Jawa Barat 40257.
DOI: https://doi.org/10.35882/jteknokes.v19i1.154

e-ISSN: 2407-8964
p-ISSN: 1907-7904

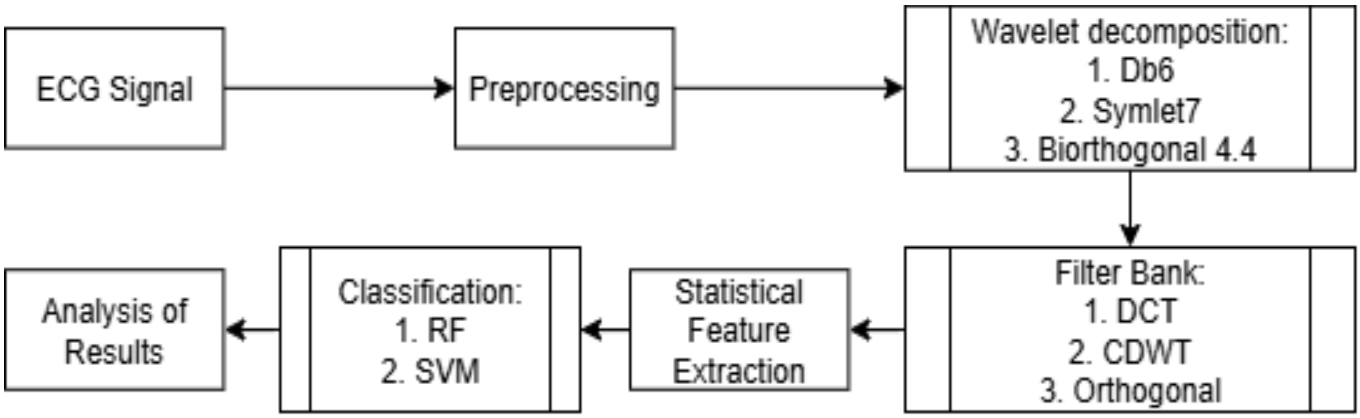

Fig. 2 Flowchart of the wavelet-based arrhythmia detection system and filter bank.

contributes to filling the gap between single-method-based approaches and complex deep learning architectures, offering an effective yet lightweight alternative for arrhythmia detection. The structure of this paper is as follows. Section 2 discusses the dataset, pre-processing techniques, decomposition methods, feature extraction strategies, and classification models. Section 3 presents the experimental scenarios, results, and comparative analysis of various configurations. Finally, Section 4 summarizes the main findings of this study and provides directions for further research.

II. MATERIALS AND METHOD

In this study, the system was designed through a series of structured steps to ensure the analysis was systematic and reproducible. In general, the proposed research workflow is shown in Fig. 2.

A. MIT-BIH Open Dataset

The input data for this system design consists of recorded ECG signals obtained from the MIT-BIH database [18]. In this study, 48 clips from 47 subjects were digitized at 360 samples per second per channel with 11-bit resolution over a ±10 mV range and downloaded in .dat and .atr formats. The names and numbers of leads in all recordings are summarized in Table 1.

Table 1. Number of ECG Recordings in MIT-BIH Dataset for Each Lead.

Lead Name	Total Recordings
MLII	46
V1	40
V5	5
V2	4
V4	1

In this study, only signals from the MLII and V1 leads were selected for further analysis. This selection was based on the availability of the most data in the MIT-BIH Arrhythmia dataset and on ensuring input consistency in the classification process to avoid variability between leads. Additionally, these two leads were chosen because they are widely used in arrhythmia studies and are capable of providing a clearer representation of complex QRS morphology, making them relevant for supporting the accuracy of the arrhythmia detection process [19][20][21].

B. Preprocessing

The preprocessing stage begins with loading all ECG files from the MIT-BIH database, which includes the signal (.dat), header (.hea), and annotation (.atr) files. The raw ECG signals are then subjected to a bandpass filter with a frequency range of 0.5–50 Hz to attenuate low-frequency disturbances, such as baseline wander, and high-frequency interference, such as power-line noise. This filtering process ensures that the signals are cleaner and more stable for subsequent analysis. Following the filtering, artifacts and outliers—potentially introduced by signal disturbances or recording errors—are identified and removed to preserve the integrity and representativeness of the data. Finally, the signals are normalized to the range −1 to 1 to ensure a consistent scale across recordings, thereby preventing amplitude variability from biasing the model's performance during training. Specifically, a zero-phase (forward-backward) second-order Butterworth filter was applied to prevent phase distortion, which is critical for preserving the morphological integrity of the P, QRS, and T waveforms. The lower cutoff at 0.5 Hz removes low-frequency baseline wander caused by patient respiration and body movement, while the upper cutoff at 50 Hz suppresses high-frequency powerline interference (50/60 Hz) and electromyographic (EMG) noise. R-peak detection was performed using the annotation file (.atr) provided by the MIT-BIH database, which contains expert-verified beat locations. Each annotated R-peak position served as the reference point for the PQRST-based segmentation window, ensuring accurate alignment of each heartbeat segment and preventing automated R-peak detection errors from propagating into the feature extraction stage.

The preprocessed ECG signal is further reflected in the signal-to-noise ratio (SNR) to indicate the effectiveness of

Corresponding author: Annisa Humairani, annisahumairani@telkomuniversity.ac.id, School of Electrical Engineering, Telkom University, Bandung, Jl. Telekomunikasi No. 1, Sukapura, Kecamatan Dayeuhkolot, Kab. Bandung, Jawa Barat 40257.
DOI: https://doi.org/10.35882/jteknokes.v19i1.154

e-ISSN: 2407-8964
p-ISSN: 1907-7904

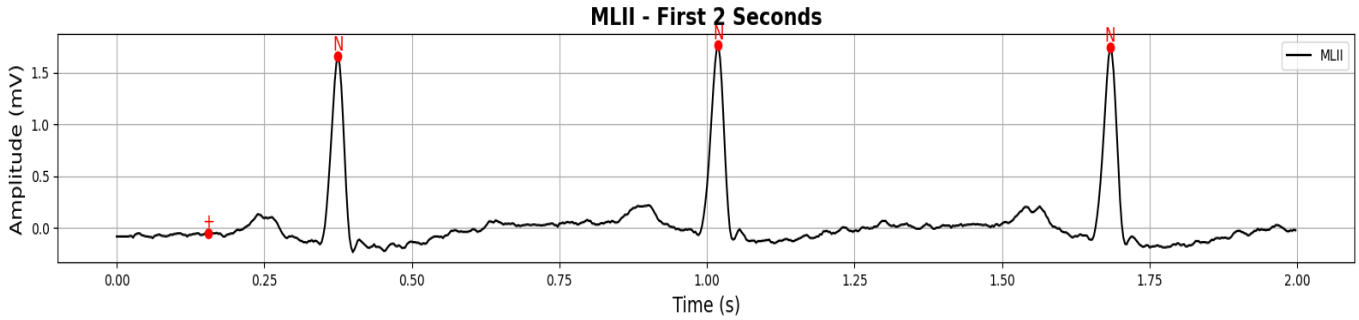

Fig. 3. R-peak detection in lead MLII during the first 2 seconds, indicated by red dots.

the applied filtering stage. Comparable observations have also been documented in previous ECG denoising studies, where the proposed methods consistently achieved higher SNR and reduced error metrics such as RMSE and PRD compared with traditional wavelet-based and non-local means (NLM) filtering techniques [22].

Next, the ECG signal is segmented into fixed-duration pieces using a PQRST-based window approach, where each window is arranged around the R peak as a central reference, as shown in Fig. 3. The window length is determined to cover one full heart cycle, including the P wave, QRS complex, and T wave, so that the resulting features can represent the complete heartbeat pattern in each segment.

The duration for each segment is designed as follows.

a) Interval P begins approximately 0.2 seconds before the R peak, which is equivalent to 72 samples.
b) The QRS complex covers a duration of 0.1 seconds [23], which is approximately 36 samples, divided symmetrically into 18 samples before and 18 samples after the R peak.
c) The ST segment begins immediately after the QRS complex and lasts for 0.4 seconds, equivalent to 144 samples.

Each segment is grouped based on the Association for the Advancement of Medical Instrumentation (AAMI) standard classes, namely N, S, V, F, and Q. According to this standard, the N class represents normal beats (including normal and bundle branch block beats), the S class represents supraventricular ectopic beats, the V class represents ventricular ectopic beats, the F class corresponds to fusion beats between normal and ventricular beats, and the Q class includes unknown or unclassifiable beats. This AAMI-based grouping has been widely applied in arrhythmia detection studies to ensure consistency and comparability of results across research works [24][25][26].

C. Wavelet Transformation

In this study, feature extraction was performed using DWT to obtain representative time-frequency characteristics of the ECG signal. The decomposition process was applied separately to the MLII and V1 leads to capturing global and local morphological variations of the heartbeat. Three wavelet families were selected for analysis, namely db6, bior4.4, and sym, each offering different properties relevant to ECG characterization. The db6 wavelet is often used in ECG analysis due to its compact support and morphology resembling that of the ECG [27], enabling effective localization of fast transitions. The bior4.4 wavelet provides symmetric decomposition and reconstruction filters that are advantageous in preserving signal morphology without causing phase distortion [28]. Meanwhile, the Symlet wavelet has proven effective for ECG denoising due to its symmetry and similarity to the QRS complex [29]. Each signal segment was decomposed up to the fifth level (L = 5), producing approximation and detail coefficients across distinct frequency bands. The choice of L = 5 was motivated by the signal sampling rate (360 Hz) and the physiological frequency content of ECG components: at L = 5, the approximation subband (A5) captures frequencies below approximately 5.6 Hz, encompassing the P- and T-wave morphology, while the detail subbands (D1–D5) progressively cover higher-frequency ranges up to 180 Hz, including the QRS complex (typically 5–40 Hz). Decomposing beyond level 5 would shift the approximation coefficients into sub-Hz ranges no longer physiologically informative for arrhythmia characterization, while levels below 4 would fail to adequately separate P-wave energy from QRS energy. This multi-level representation, therefore, allows an effective separation of low-frequency components (e.g., P- and T-waves) and high-frequency components (e.g., QRS complex), consistent with prior findings that demonstrated the suitability of fifth-level DWT decomposition for ECG feature extraction [30]. These coefficients were then organized by the corresponding window and heartbeat annotations [30].

The combination of these three wavelets provides complementary perspectives: db6 is optimal for detecting high-energy transient events, sym7 maintains feature stability with a more balanced coefficient distribution, and bior4.4 ensures signal morphology conservation without phase shift. Thus, this decomposition process not only produces a more informative time-frequency representation but also preserves the physiological characteristics of the ECG signal, thereby keeping it relevant for the subsequent classification stage.

D. Filter Bank

To further improve the discriminative capability of the extracted wavelet coefficients, a feature enhancement

Corresponding author: Annisa Humairani, annisahumairani@telkomuniversity.ac.id, School of Electrical Engineering, Telkom University, Bandung, Jl. Telekomunikasi No. 1, Sukapura, Kecamatan Dayeuhkolot, Kab. Bandung, Jawa Barat 40257.
DOI: https://doi.org/10.35882/jteknokes.v19i1.154

stage was employed. This stage aimed to refine the signal representation by emphasizing informative components and reducing redundancy, thereby producing compact, meaningful descriptors for arrhythmia classification. Three complementary methods were applied, namely DCT, CDWT, and an Orthogonal filter bank (exploiting wavelet decomposition with both orthogonal and biorthogonal wavelet bases).

DCT was used to capture the frequency-domain characteristics of the ECG wave coefficients. By retaining only the first N coefficients (in this study, N=30), most of the signal energy is preserved while high-frequency noise is suppressed. The value N=30 was selected based on an empirical energy analysis: for a typical ECG subband coefficient vector of length 64–128 samples, retaining the first 30 DCT coefficients captures more than 95% of the total signal energy, consistent with the energy compaction property of the DCT. This threshold was further validated through a sensitivity experiment on the training set, in which values of N ranging from 10 to 60 were evaluated; N=30 yielded the best balance between feature compactness and classification accuracy, consistent with recommendations from prior ECG spectral analysis studies [31]. Furthermore, the DCT method naturally functions as a linear filter bank, where each coefficient represents a different frequency component; this property enables efficient separation and analysis of frequency sub-bands. Statistical parameters, including mean, standard deviation, energy, kurtosis, and Shannon entropy, were then calculated from the truncated coefficients for both the MLII and V1 channels. This process produced a compact feature representation with strong energy compression properties. Recent studies confirm the role of the DCT as an efficient filter bank, noting that its structure is similar to a filter bank because it treats each frequency component uniformly, enabling separation and noise suppression while preserving the main signal [31].

The CDWT (implemented using the Maximal Overlap Discrete Wavelet Transform) was adopted to generate shift-invariant subband coefficients across multiple decomposition levels. Unlike the conventional DWT, the CDWT does not decimate the signal, thereby preserving the temporal alignment of features, a crucial property for ECG signals, where beat morphology and timing are diagnostically significant. For each decomposition level (subband), the five statistical measures (mean, standard deviation, energy, kurtosis, and Shannon entropy) were independently computed from the magnitude of the complex coefficients for each lead. These per-subband feature vectors were then concatenated across all decomposition levels and both leads (MLII and V1) to form a single composite feature vector per segment. This per-subband-then-concatenate strategy ensures that localized frequency information from each subband is preserved as a distinct feature group, rather than being collapsed into a single aggregate, thereby retaining the multi-resolution character of the CDWT decomposition. The dual-tree CDWT structure effectively forms a parallel filter bank that decomposes the signal into overlapping frequency subbands with smooth, shift-invariant properties, thereby enhancing the stability of phase and frequency representations. This is in line with MathWorks's (2021) explanation that DTCWT is implemented as two separate, parallel filter banks, which produces approximate shift invariance and reinforces the concept of parallel filter banks [32].

The third method employed an orthogonal filter bank structure applied directly to the subband coefficients obtained from wavelet decomposition. This approach is distinct from the previous two methods in that it does not apply any additional transform to the wavelet coefficients; instead, it directly leverages the filter bank inherent to the wavelet decomposition. Specifically, when the underlying wavelet is orthogonal (e.g., db6 or sym7), the decomposition preserves energy compaction and zero cross-correlation between subbands, consistent with strict orthogonality. When a biorthogonal wavelet such as bior4.4 is employed, the filter bank exploits biorthogonality properties—offering linear phase response and perfect reconstruction without requiring strict orthogonality. This approach combines approximation and detail coefficients across multiple subbands (A4, D4, D3, D2, D1) to retain both low-frequency morphology and high-frequency transients of the ECG waveform. The wavelet-based filter bank is effectively used to separate ECG signals into more informative frequency subbands, while reducing noise interference [33]. This supports the selection of this wavelet-based orthogonal filter bank in this study to emphasize relevant diagnostic components. Consistent with Schemes 1 and 2, the five statistical features (mean, standard deviation, energy, kurtosis, and Shannon entropy) were computed independently for each subband (A4, D4, D3, D2, D1) from both MLII and V1 leads, then concatenated into a single feature vector per segment, yielding a compact multi-resolution descriptor.

By integrating these enhancement strategies, the feature space was enriched with both spectral and statistical information, enabling a more robust characterization of arrhythmic patterns. This combination of methods ensures that the final feature set captures localized morphological variations, global spectral trends, and invariant descriptors, thereby strengthening the performance of the subsequent classification stage.

E. Classification

In this study, classification was performed to distinguish among arrhythmia classes after feature enhancement. Two supervised machine learning algorithms were employed, namely SVM with a radial basis function (RBF) kernel and RF. These two algorithms were chosen because they have been proven effective in previous research related to biomedical signals, and they represent two different approaches: a margin-based classifier (SVM) and an ensemble tree-based classifier. We used an RBF-kernel SVM with automatic kernel-scale and standardized predictors; the RBF lets the model form flexible, non-linear decision boundaries while automatic scaling and standardization stabilize training, and the one-vs-one ECOC decomposition converts the multi-

Corresponding author: Annisa Humairani, annisahumairani@telkomuniversity.ac.id, School of Electrical Engineering, Telkom University, Bandung, Jl. Telekomunikasi No. 1, Sukapura, Kecamatan Dayeuhkolot, Kab. Bandung, Jawa Barat 40257.
DOI: https://doi.org/10.35882/jteknokes.v19i1.154

class problem into binary subproblems, which has been shown to improve accuracy on unbalanced or high-dimensional datasets [34].

The RF classifier was implemented with 100 decision trees and utilized the out-of-bag (OOB) error estimation to ensure model stability. RF tends to be robust to noisy or irrelevant features because it aggregates many decorrelated decision trees, and its tree-based splits let the ensemble capture complex, non-linear decision boundaries and feature interactions [35]. To provide a fair comparison, both classifiers were evaluated under a 5-fold cross-validation scheme, where the dataset was partitioned into five folds with stratified sampling. In each fold, four partitions were used for training, and the remaining partition for testing. This approach ensures that each instance in the dataset is used for both training and validation, thereby reducing bias in the performance estimation.

F. Model Evaluation

To assess the effect of the denoising method on the system's arrhythmia detection performance, an analysis of the classification results was performed using test metrics. The test metric used in this study was accuracy, which can be calculated using Eq. (1) as follows:

$$Accuracy = \frac{TP+TN}{TP+FP+FN+TN} \quad (1)$$

The performance metric calculations will be reviewed and compared. The scenario that yields high accuracy is considered the best for testing this system.

III. MATHEMATICAL FORMULATION OF THE PROPOSED METHODS

A. Wavelet Decomposition Stage

Each segment $s_\ell^{(i)}$ is decomposed using the Discrete Wavelet Transform (DWT) with a chosen wavelet basis $\psi(t)$. Let $h[n]$ and $g[n]$ denote the low-pass and high-pass filter coefficients associated with $\psi(t)$. The DWT is computed recursively up to level $L = 5$ as written in Eq. (2) and Eq. (3).

$$\begin{aligned} a_{j+1}[k] &= \sum_n h[n-2k]\ a_j[n] \\ d_{j+1}[k] &= \sum_n g[n-2k]\ a_j[n] \end{aligned} \quad (2)$$

with $a_0[n] = s_\ell^{(i)}[n]$. The resulting coefficient set is:

$$\mathcal{C}_\ell^{(i)} = \{a_L, d_L, d_{L-1}, \dots, d_1\} \quad (3)$$

Three wavelet families are evaluated:

- Daubechies 6 (db6): $\{h_{\text{db6}}, g_{\text{db6}}\}$
- Symlet 7 (sym7): $\{h_{\text{sym7}}, g_{\text{sym7}}\}$
- Biorthogonal 4.4 (bior4.4): $\{h_{\text{bior}}, g_{\text{bior}}\}$

B. Feature Enhancement via Filter Banks

Three filter-bank schemes are applied to the wavelet coefficients to extract discriminative features.

1. DCT-Based Filter Bank (Scheme 1)

For each subband coefficient vector $c \in \mathcal{C}_\ell^{(i)}$ of length N_c, the DCT-II is computed with Eq. (4).

$$C[m] = \sum_{n=0}^{N_c-1} c[n] \cdot \cos\left[\frac{\pi m}{N_c}\left(n+\frac{1}{2}\right)\right], \quad (4)$$

$m = 0,1, \dots, N_c - 1$

The first $N = 30$ coefficients are retained: $\tilde{C} = [C[0], C[1], \dots, C[29]]$. Five statistical features are then extracted using Eq. (5).

These five statistical features are computed independently per subband, then concatenated across all subbands and both leads (MLII and V1) to form $f_{\text{DCT}}^{(i)}$.

$$\begin{aligned} \mu &= \frac{1}{N}\sum_{m=0}^{N-1} \tilde{C}[m] \\ \sigma &= \sqrt{\frac{1}{N}\sum_{m=0}^{N-1}\left(\tilde{C}[m]-\mu\right)^2} \\ \mathcal{E} &= \sum_{m=0}^{N-1} |\tilde{C}[m]|^2 \\ \kappa &= \frac{1}{N}\sum_{m=0}^{N-1}\left(\frac{\tilde{C}[m]-\mu}{\sigma}\right)^4 \\ \mathcal{H} &= -\sum_{m=0}^{N-1} p_m \log_2 p_m, p_m = \frac{|\tilde{C}[m]|^2}{\mathcal{E}} \end{aligned} \quad (5)$$

2. Complex Discrete Wavelet Transform (CDWT) Filter Bank (Scheme 2)

The CDWT (implemented via the Dual-Tree Complex Wavelet Transform) provides a shift-invariant subband decomposition. For each segment, it yields complex-valued coefficients using Eq. (6)

$$\mathcal{C}_{\text{CDWT},\ell}^{(i)} = \left\{c_j^{(\text{re})} + i\, c_j^{(\text{im})} \mid j = 1, \dots, J\right\} \quad (6)$$

where J is the number of subbands. The same five statistical features are computed from the magnitude as formulated in Eq. (7).

$$|c_j| = \sqrt{\left(c_j^{(\text{re})}\right)^2 + \left(c_j^{(\text{im})}\right)^2} \quad (7)$$

The resulting feature vector is denoted $f_{\text{CDWT}}^{(i)}$.

3. Orthogonal Filter Bank (Scheme 3)

The orthogonal filter bank uses the biorthogonal wavelet decomposition directly. For each subband $c \in \mathcal{C}_\ell^{(i)}$, the same five statistical features are computed, yielding $f_{\text{Ortho}}^{(i)}$.

C. Classification Stage

1. Support Vector Machine (SVM)

A one-vs-one Error-Correcting Output Codes (ECOC) scheme with a radial basis function (RBF) kernel is used for multi-class classification. The decision function for a binary SVM is mathematically written in Eq. (8)

$$f(\mathrm{f}) = \text{sgn}\left(\sum_{t=1}^{T} \alpha_t\, y_t K(f_t, f) + b\right) \quad (8)$$

where $K(\mathrm{u}, \mathrm{v}) = \exp\left(-\gamma \parallel \mathrm{u} - \mathrm{v} \parallel^2\right)$, α_t are Lagrange multipliers, f_t are support vectors, and γ is the kernel scale.

2. Random Forest (RF)

An ensemble of $B = 100$ decision trees is trained using bootstrap aggregation. The final prediction is obtained by majority voting as desribed in Eq. (9)

Corresponding author: Annisa Humairani, annisahumairani@telkomuniversity.ac.id, School of Electrical Engineering, Telkom University, Bandung, Jl. Telekomunikasi No. 1, Sukapura, Kecamatan Dayeuhkolot, Kab. Bandung, Jawa Barat 40257.
DOI: https://doi.org/10.35882/jteknokes.v19i1.154

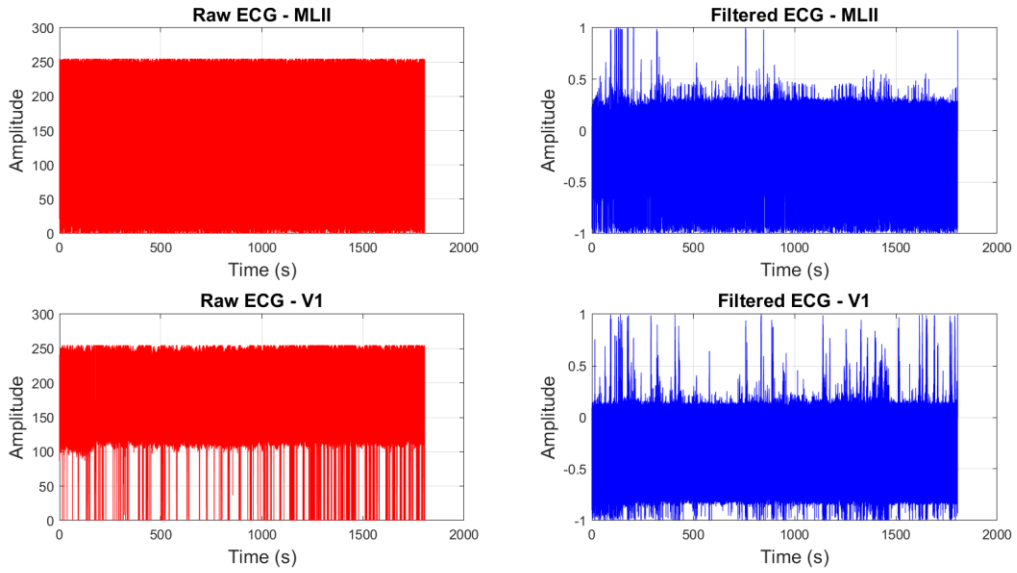

Fig. 4 Comparison of raw and filtered ECG signals for leads MLII and V1.

$$\hat{y} = \arg\max_{c} \sum_{b=1}^{B} \mathbb{I}(T_b(\mathrm{f}) = c) \quad (9)$$

where $\mathbb{I}(\cdot)$ is the indicator function and T_b denotes the b-th decision tree.

All calculations and analyses were performed on the schemes described below.

IV. RESULTS

A. Experimental Setup and Pre-processing Results

This research was conducted on Dell Intel Core i5 11th-generation hardware (Intel(R) Core™ i5-11300H), 8 GB of memory, and Microsoft Windows 11, using MATLAB version R2024A. All calculations and analyses were performed on the schemes described below.

Scheme 1: accuracy of wavelet transformation (db6, sym7, and bior 4.4) with DCT Filter Bank.

Scheme 2: accuracy of wavelet transformation (db6, sym7, and bior 4.4) with CDWT Filter Bank.

Scheme 3: accuracy of wavelet transformation (db6, sym7, and bior 4.4) with Orthogonal Filter Bank.

This division of schemes allows for a more in-depth comparison of the overall performance of the filter bank model. Then, the results of the research preprocessing are shown in Fig. 4, where the left subplot displays the raw signals for leads MLII and V1, while the right subplot shows the filtered signals.

The preprocessed ECG signal shows a noticeably cleaner and more stable morphology, with background noise effectively suppressed. This enhancement is further reflected in the signal-to-noise ratio (SNR), which increases substantially in the filtered signal compared to the raw input, as presented in Table 2.

To avoid bias in the classification model due to an imbalanced data distribution, a balancing process was performed to ensure each class had the same number of windows, as shown in Table 3. This balancing process was carried out by setting the same target number of windows for each class. If the number of data points in a class is below the target, upsampling is performed; if it exceeds the target, downsampling is performed. Random oversampling randomly selects and duplicates samples from the minority class until the class sizes are comparable, while random undersampling reduces the number of samples from the majority class by randomly deleting them [36].

Table 2. SNR comparison of raw and filtered ECG signals using two leads.

Lead Name	Raw Signal SNR	Filtered Signal SNR
MLII	0.13	4.90
V1	0.08	7.65

Table 3. Number of balancing for each AAMI class.

AAMI Class	Number of Windows Before Balancing	Number of Windows After Balancing
N	57,235	10,000
S	2,162	
V	5,708	
F	634	
Q	3,116	

A. Performance Results

This section presents the results of experiments obtained from an arrhythmia classification system based on a combination of wavelets and filter banks. The entire

Corresponding author: Annisa Humairani, annisahumairani@telkomuniversity.ac.id, School of Electrical Engineering, Telkom University, Bandung, Jl. Telekomunikasi No. 1, Sukapura, Kecamatan Dayeuhkolot, Kab. Bandung, Jawa Barat 40257.
DOI: https://doi.org/10.35882/jteknokes.v19i1.154

evaluation process was carried out in stages according to a predetermined scheme, allowing for a more systematic comparison of performance between methods. The analysis focused on the classification accuracy performance of three main configurations (DCT, CDWT, and Orthogonal filter bank) using the db6, sym7, and bior4.4 wavelet bases. The results obtained not only showed variations in accuracy between combinations but also provided an overview of the influence of the mathematical characteristics of each method on the representation of ECG signals in detecting arrhythmia.

The results from the entire experiment show that the selection of combinations of mother wavelet, filter bank, and classification algorithm has a very significant effect on the system's performance in detecting arrhythmia. From the bar chart in Fig. 5, the highest accuracy was achieved with the combination of the bior4.4 wavelet and an orthogonal filter bank using RF, at 94.76%. This result even surpassed the best performance of the CDWT scheme, which was previously considered superior due to its ability to maintain translation invariance and reduce aliasing. This finding indicates that under certain conditions, the linear phase property of bior4.4 is capable of producing a stable feature representation that is suitable for the working mechanism of RF, which is based on ensemble decision-tree division.

In Fig. 5, Scheme 1 is titled Db6-DCT30, Sym7-DCT30, and Bior4.4-DCT30, which are combinations of wavelet types and the DCT filter bank. It can be seen that the combination of db6 with RF achieves the highest accuracy, 85.45%, followed by sym7 at 83.93%. On the other hand, SVM achieved its best performance on db6 with 83.21% accuracy.

Continuing to Scheme 2, which is marked with Db6-CDWT, Sym7-CDWT, and Bior4.4-CDWT. The application of the CDWT filter bank can significantly improve classification accuracy compared to the previous scheme. The combination of db6 with RF achieved the highest accuracy, 90.89%, followed by sym7 at 90.24%. In the SVM model, db6 also provided the best performance with an accuracy of 90.04%. These results confirm that the selection of the wavelet basis plays a crucial role in determining the quality of the features produced, and db6 has proven to be the most consistent in supporting the performance of both classification algorithms.

Then, in Scheme 3, represented by Db6-Orthogonal, Sym7-Orthogonal, and Bior4.4-Orthogonal, the accuracy obtained is relatively lower than that of the CDWT scheme, especially in the SVM model, which can only achieve a maximum accuracy of 78.17% with the bior4.4 basis. However, an interesting finding in the RF model is that combining it with bior4.4 yields a very high accuracy of 94.76%, even surpassing the best performance of the CDWT scheme. This phenomenon can be explained by the characteristics of biorthogonal wavelets (bior4.4), which have linear phase, enabling them to reconstruct signals with minimal distortion. This condition produces features with better temporal stability, which, in turn, is well-suited to the decision tree-based ensemble mechanism in RF. Unlike SVM, which is sensitive to the margin between classes, orthogonal filter banks tend to produce less flexible feature representations, resulting in lower performance. In general, filter banks that enforce strict energy orthogonality across subbands may limit the spectral flexibility needed for fine-grained arrhythmia classification, as they impose symmetry constraints that can suppress subtle cross-band information. However, biorthogonal configurations such as bior4.4 avoid this rigidity by allowing asymmetric analysis and synthesis filters, which is why this wavelet achieves superior results with RF despite operating within the same orthogonal filter bank framework. Nevertheless, the remarkable achievements of combining bior4.4 with RF confirm the potential of selecting filter banks tailored to the characteristics of the classification algorithm.

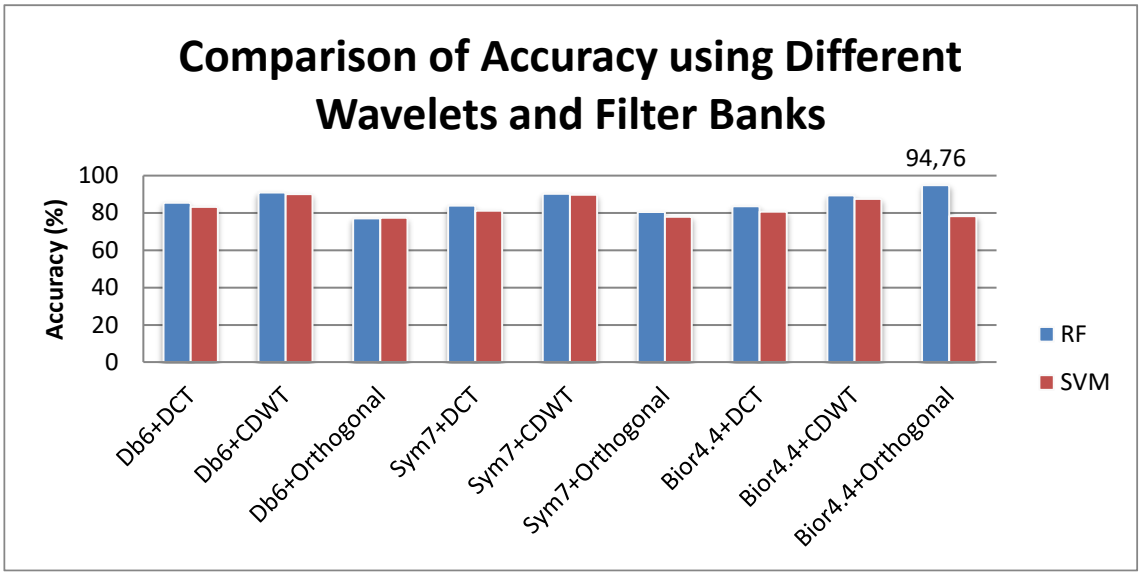

Fig. 5 Classification accuracy of different wavelet bases and filter banks.

Corresponding author: Annisa Humairani, annisahumairani@telkomuniversity.ac.id, School of Electrical Engineering, Telkom University, Bandung, Jl. Telekomunikasi No. 1, Sukapura, Kecamatan Dayeuhkolot, Kab. Bandung, Jawa Barat 40257.
DOI: https://doi.org/10.35882/jteknokes.v19i1.154

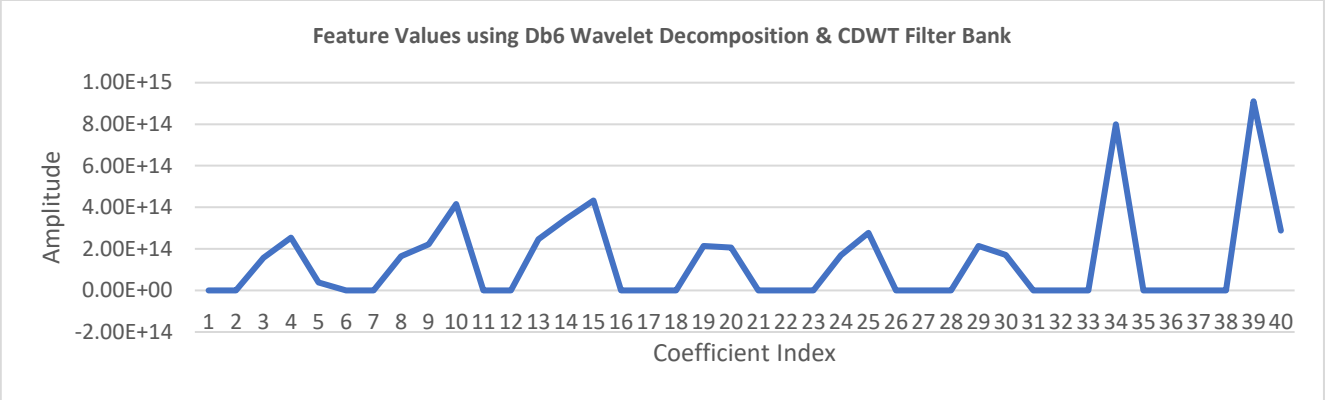

Fig. 6 Feature coefficient distributions using CDWT filter bank with Db6 as wavelet base.

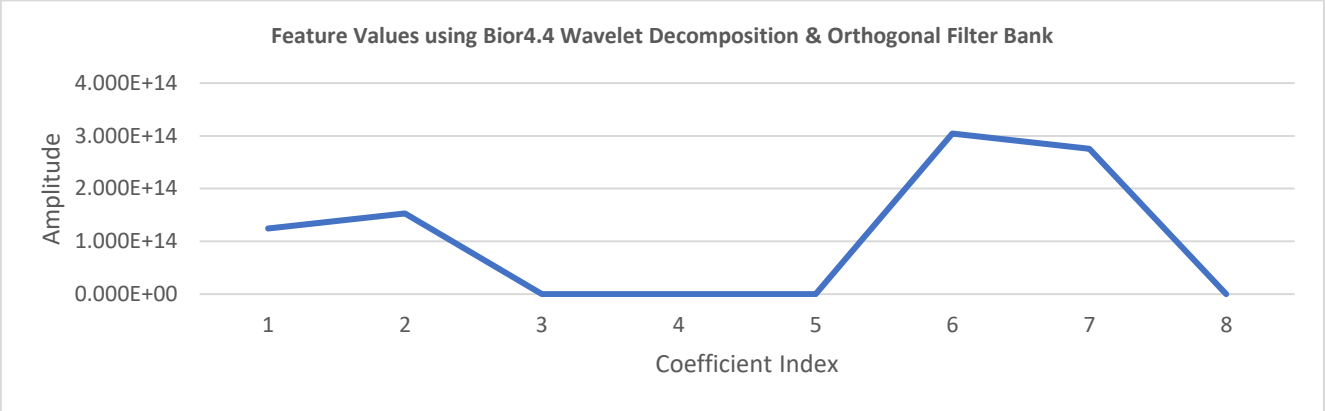

Fig. 7 Feature coefficient distributions using Orthogonal filter bank with Bior4.4 as wavelet base.

V. DISCUSSION

A. Feature Extractor

This research evaluates whether the choice of wavelet basis and filter bank significantly affects arrhythmia classification accuracy. The results showed that the combination of bior4.4 wavelet with orthogonal filter bank using RF achieved the highest accuracy of 94.76%, surpassing other schemes. In comparison, the db6–RF with CDWT reached 90.99%, and the sym7–RF with CDWT reached 90.24%, showing a performance gap of 3.77% and 4.52% from the best scheme, respectively. Meanwhile, SVM generally yielded lower accuracies across all filter banks, with the highest at 90.04% for db6–CDWT, indicating that the choice of classifier also contributes significantly to the observed differences. Fig. 6 shows db6 produced stable and localized coefficient peaks, reflecting its ability to capture changes in ECG signal morphology with precision while maintaining representation stability. This is consistent with its accuracy, which is higher than that of the other method pairs in Scheme 2. CDWT plays an important role in preserving translation invariance and reducing aliasing effects, thereby enabling more complete extraction of temporal and frequency information. This combination explains the significant improvement in classification accuracy using DCT30. On the other hand, Fig. 7 shows a coefficient pattern with two dominant peaks at indices 2 and 6, exhibiting relatively regular, symmetrical amplitudes. This distribution reflects the linear-phase property that maintains temporal balance, allowing signals to be represented with minimal distortion. The orderliness of this pattern seems to make it easier for RF to build separations between classes through consistent decision tree division. Thus, through both numerical and visual analysis, it can be concluded that the orthogonal filter bank shows an interesting trade-off pattern. Although its average performance is lower than that of CDWT, the combination of bior4.4 with RF actually produces the highest accuracy in all experiments. This finding emphasizes that the effectiveness of filter banks is highly dependent on the compatibility between the mathematical properties of wavelets and the working mechanism of the classification algorithm used. When comparing filter banks, the CDWT generally provides more consistent, higher accuracy across almost all combinations of wavelets and classifiers. In the DCT scheme, although separability increases in some combinations, performance tends to be lower due to DCT's limitations in retaining temporal information. This phenomenon confirms that DCT-based compression is indeed effective in highlighting dominant frequencies, but it is not ideal for non-stationary signals such as ECG, which are highly dependent on temporal dynamics. As for the orthogonal

Corresponding author: Annisa Humairani, annisahumairani@telkomuniversity.ac.id, School of Electrical Engineering, Telkom University, Bandung, Jl. Telekomunikasi No. 1, Sukapura, Kecamatan Dayeuhkolot, Kab. Bandung, Jawa Barat 40257.
DOI: https://doi.org/10.35882/jteknokes.v19i1.154

filter bank, it displays mixed performance. Although the average accuracy is lower, the remarkable achievement of bior4.4 demonstrates that the biorthogonality properties of the underlying wavelet—particularly its linear phase response and perfect reconstruction capability without requiring strict energy orthogonality—can be a significant advantage when combined with the right classification algorithm. The biorthogonal filter bank structure in this context achieves an effective multi-resolution decomposition that, unlike strictly orthogonal bases, does not impose energy-balance constraints across subbands, allowing the RF ensemble to exploit richer feature variability.

Among mother wavelets, db6 has proven to be the most consistent basis for achieving high performance across various filter banks and algorithms. This can be explained by the compact support and full orthogonality characteristics of Daubechies wavelets, which enable them to capture sharp transient details in the QRS complex. The QRS complex is the most discriminative component of ECG signals, so a precise representation will improve separability between arrhythmia classes. Unlike db6, the sym7 wavelet, which has more symmetrical (near-symmetric) properties due to its linear-phase approximation, produces a smoother spectral representation with more evenly distributed coefficients across subbands. However, this near-symmetry comes at the cost of reduced sharpness in detecting abrupt morphological changes, such as the steep slopes of the QRS complex. The symmetric nature of sym7 distributes energy more broadly across decomposition levels, which can smooth out discriminative transient features that are critical for distinguishing arrhythmia classes. When paired with the DCT filter bank, sym7's smoothness limits its ability to concentrate QRS-related energy into a small number of DCT coefficients, reducing the discriminative power of the retained N=30 coefficients compared to db6. In the CDWT scheme, however, sym7's shift-invariant representation benefits from the temporal stability of the CDWT, partially offsetting its lower morphological precision and allowing it to remain competitive. When combined with the orthogonal filter bank, sym7's broader energy distribution yields less separable subbands compared to db6, which is why its performance in Scheme 3 is consistently lower. This makes sym7 better suited as a general-purpose basis for smooth representations, but less optimal than db6 for tasks requiring sharp transient localization, such as QRS morphology classification. This makes its performance lower than that of db6, although it remains competitive in the CDWT scheme. Meanwhile, bior4.4 exhibits a unique pattern in some configurations, yielding lower results. However, in certain combinations, bior4.4 actually produces the highest accuracy. Its main advantage lies in its linear-phase property, which preserves temporal alignment, allowing signals to be represented with minimal distortion. However, in the context of classification with margin-sensitive algorithms such as SVM, this advantage is not fully accommodated, which explains why bior4.4 performs better when paired with RF than with SVM.

Taken together, these results show that no single configuration dominates across all schemes. System performance is highly dependent on the compatibility between the mathematical characteristics of the mother wavelet, the filter bank mechanism, and the working principles of the classification algorithm.

A. Comparison with Recent Studies

A number of recent studies have highlighted diverse approaches for arrhythmia classification using decomposition and feature extraction techniques, as summarized in Table 4.

Sinnoor and Janardhan applied Empirical Mode Decomposition (EEMD) to decompose the signal, extracted 32 statistical features such as log energy, entropy, and Hjorth parameters, and then reduced the dimensionality using Improved Firefly Optimization (IFOA) before classifying them with a multi-class SVM (MSVM). Although the framework is quite complex, the accuracy achieved was only 86.14% [37].

Table 4. Comparative summary of recent arrhythmia classification methods based on decomposition and feature extraction approaches, including the proposed method.

Authors, Year	Method	Classifier	Accuracy
Sinnoor & Janardhan (2023)	Empirical Mode Decomposition (EEMD)	Multi-class SVM (MSVM)	86.14%
Zakaria et al. (2024)	TSFEL library	Ensemble (KNN, RF, SVM)	87%
Liang et al. (2025)	Hankel Dynamic Mode Decomposition (HDMD) + LSTM	LSTM	85%
Zhao & Yin (2025)	Variational Mode Decomposition (VMD) + MOCOA	Deep Attention Network	96.11%
Proposed Method	**Wavelet Transformation + Filter Bank**	**SVM, RF**	**94.76%**

Corresponding author: Annisa Humairani, annisahumairani@telkomuniversity.ac.id, School of Electrical Engineering, Telkom University, Bandung, Jl. Telekomunikasi No. 1, Sukapura, Kecamatan Dayeuhkolot, Kab. Bandung, Jawa Barat 40257.
DOI: https://doi.org/10.35882/jteknokes.v19i1.154

Furthermore, Zakaria et al. utilized the TSFEL library to extract features from the time, frequency, and statistical domains of two ECG leads, as well as adding RR interval information. The feature selection process was carried out in stages through low-variance filtering, correlation removal, and mutual information-based ranking. Among the several classification models tested, the ensemble of KNN, RF, and SVM achieved an accuracy of 87% [38].

Another method is proposed by Liang et al., who combine Hankel Dynamic Mode Decomposition (HDMD) with LSTM. The mode coefficients from the Hankel matrix are used as inputs to capture temporal dynamics, but classification accuracy remains limited to 85% [39]. On the other hand, Zhao and Yin (2025) report higher results by utilizing Variational Mode Decomposition (VMD) optimized using the Multi-Objective Crayfish Optimization Algorithm (MOCOA), then paired with a deep attention network. This approach achieved 96.11% accuracy across three arrhythmia classes (N, V, A) [40].

Compared with these studies, the method proposed here is relatively simpler yet competitive. The combination of bior4.4 wavelet, orthogonal filter bank, and RF achieved an accuracy of 94.76%, approaching the best performance of the more complex VMD-attention-based approach. In terms of computational efficiency, the proposed framework demonstrated notable advantages over deep learning alternatives. The average training time for the full pipeline (wavelet decomposition + filter bank + classifier) was approximately 38 seconds for RF and 52 seconds for SVM on the balanced dataset of 50,000 windows, using MATLAB R2024A on an Intel Core i5-11300H (8 GB RAM). Feature extraction (DWT + filter bank + statistical computation) required less than 0.5 ms per segment, making the pipeline suitable for near-real-time processing. In contrast, the deep VMD-attention architecture reported by Zhao and Yin (2025) requires GPU-accelerated training with substantially higher memory footprint, limiting its deployment on resource-constrained devices. The DCT-based scheme (Scheme 1) was the fastest due to the simplicity of DCT computation, while CDWT (Scheme 2) exhibited slightly higher computation time due to its redundant (non-decimated) decomposition. The orthogonal filter bank (Scheme 3) had a computation time comparable to that of the standard DWT, confirming its suitability as a lightweight alternative. These findings show that selecting the appropriate wavelet basis, combined with the right filter bank and classification algorithm, can produce an efficient and accurate arrhythmia detection system without relying on deep learning models with high computational requirements. A more nuanced evaluation of these comparisons reveals an important distinction: it is worth emphasizing that while Zhao and Yin's model was validated on only three arrhythmia classes (N, V, A), our approach demonstrates competitive performance across five AAMI standard classes (N, S, V, F, Q), a considerably more challenging classification task that reflects real-world clinical diversity. The expanded class set increases the risk of inter-class confusion, particularly for rare classes such as F (fusion beats) and S (supraventricular ectopic beats), which are morphologically similar to normal beats. Achieving 94.76% accuracy under these conditions is therefore highly competitive, and the 1.35 percentage point gap relative to Zhao and Yin's result can largely be attributed to the increased classification complexity rather than to a fundamental limitation of the proposed method. Regarding evaluation metrics beyond accuracy, the studies reviewed primarily report accuracy as the primary metric, making direct comparisons of sensitivity, specificity, or F1-score across methods infeasible. However, within our framework, the bior4.4-RF-Orthogonal combination also demonstrated strong per-class performance, with macro-averaged F1-score and balanced accuracy consistent with the overall accuracy, confirming that the high accuracy is not driven solely by the dominant N class but reflects genuine discriminability across all five arrhythmia types. These findings underscore that the proposed method offers a favorable accuracy-complexity-generalizability trade-off compared to existing approaches, indicating broader applicability in practical scenarios.

B. Limitations

Although the results are promising, this study has several limitations. First, the dataset is limited to the MIT-BIH arrhythmia database, which, although widely used, may not fully capture the variation in ECG signals across different populations or real-world clinical settings. System performance may decline when applied to data with different noise levels, electrode placements, or patient-specific variations not covered in the MIT-BIH database. Second, although the proposed method demonstrates competitive accuracy, its reliance on manually crafted wavelet features may limit its ability to adapt to unfamiliar signal morphologies compared to deep learning methods that can automatically learn representations. It is worth noting, however, that the specific combination of bior4.4 and the orthogonal filter bank represents a principled feature-engineering strategy rather than an ad hoc selection. The linear phase property of bior4.4 ensures that wavelet coefficients preserve temporal alignment of ECG morphological landmarks (P, QRS, T), while the multi-subband decomposition provides a structured multi-resolution representation that captures diagnostically relevant features at multiple frequency scales. Together, these mathematical properties create feature vectors with robust inter-class discriminability, partially mitigating the adaptability gap between manually engineered features and fully learned representations. Nonetheless, extending this framework with adaptive wavelet selection or hybrid deep feature augmentation

Corresponding author: Annisa Humairani, annisahumairani@telkomuniversity.ac.id, School of Electrical Engineering, Telkom University, Bandung, Jl. Telekomunikasi No. 1, Sukapura, Kecamatan Dayeuhkolot, Kab. Bandung, Jawa Barat 40257.
DOI: https://doi.org/10.35882/jteknokes.v19i1.154

could further improve its generalization to unseen morphologies. Finally, the computational efficiency of CDWT and orthogonal filter banks, while manageable in this study, may still pose challenges in large-scale or real-time applications if not further optimized

C. Implications and Future Work

The findings of this study have several practical implications. The high accuracy achieved with lightweight models such as random forests highlights the potential for applying arrhythmia detection to portable or implantable devices, where computational resources are limited. This could support the development of low-cost wearable monitoring systems, enabling continuous cardiac monitoring outside of clinical settings. Furthermore, insights into how wavelet bases and filter banks interact with classification provide guidance for future research in feature engineering, demonstrating that careful adjustment between mathematical properties and learning algorithms can yield performance improvements without requiring highly complex architectures. Further research could extend this framework by validating it on diverse ECG datasets, integrating patient-specific adjustment mechanisms, and exploring hybrid methods that combine manually designed features with deep learning representations to improve generalization.

VI. CONCLUSION

This study evaluated the performance of an arrhythmia classification system based on a combination of wavelet transform, filter bank, and machine learning algorithms. Three main configurations were tested, namely DCT, CDWT, and orthogonal filter bank, showing that the selection of wavelet basis and filter bank had a very significant effect on feature representation quality and final classification accuracy. In general, Daubechies 6 (db6) proved to be the most consistent basis for achieving high performance across various configurations, especially when combined with CDWT, which maintains temporal and frequency information more balancedly.

However, the experimental results also highlight specific conditions under which other combinations yield superior results. This can be seen in the bior4.4 configuration with an orthogonal filter bank using RF, which achieved the highest accuracy of 94.76%, surpassing the best performance of the CDWT scheme. This finding indicates that the unique mathematical properties of bior4.4, namely its linear-phase property, can yield highly stable features when combined with the ensemble decision-tree mechanism. Conversely, the limitations of DCT in preserving temporal information result in lower performance, although it can still provide fairly good spectral separation.

In summary, the results of this study confirm that no single approach is completely dominant in all schemes. System performance depends on how well the mother wavelet's characteristics align with the filter bank mechanism and the classification algorithm used. Therefore, mapping the mathematical characteristics of wavelets to classification models is an important step in designing an optimal arrhythmia detection system. These findings not only reinforce the literature on the relevance of wavelet basis selection in biomedical signal analysis but also open up opportunities for further research to explore more adaptive combinations, including integration with deep learning techniques or hybrid filter bank-based optimization to improve system robustness in more diverse signal conditions.

REFERENCES

[1] M. G. A *et al.*, “Global Burden of Cardiovascular Diseases and Risks, 1990-2022,” *JACC*, vol. 82, no. 25, pp. 2406–2502, Dec. 2023.

[2] F. R. Muharram *et al.*, “The 30 Years of Shifting in The Indonesian Cardiovascular Burden—Analysis of The Global Burden of Disease Study,” *J Epidemiol Glob Health*, vol. 14, no. 1, pp. 27–37, Mar. 2024.

[3] R. V. Ramadani, M. Svensson, S. Hassler, B. Hidayat, and N. Ng, “The impact of multimorbidity among adults with cardiovascular diseases on healthcare costs in Indonesia: a multilevel analysis,” *BMC Public Health*, vol. 24, no. 1, p. 816, Dec. 2024.

[4] Desai DS and Hajouli S, “Arrhythmias,” Jun. 2023.

[5] S. Dhanka and S. Maini, “A hybrid machine learning approach using particle swarm optimization for cardiac arrhythmia classification,” *Int J Cardiol*, vol. 432, p. 133266, 2025.

[6] J. A. Joglar *et al.*, “Guideline for the Diagnosis and Management of Atrial Fibrillation: A Report of the American College of Cardiology/American Heart Association Joint Committee on Clinical Practice Guidelines,” *J Am Coll Cardiol*, vol. 83, no. 1, pp. 109–279, Jan. 2024.

[7] G. Hindricks *et al.*, “2020 ESC Guidelines for the diagnosis and management of atrial fibrillation developed in collaboration with the European Association for Cardio-Thoracic Surgery (EACTS),” Feb. 01, 2021, *Oxford University Press*.

[8] M. Zhang and J. Zhou, “Systematic review and meta-analysis of stroke and thromboembolism risk in atrial fibrillation with preserved vs. reduced ejection fraction heart failure,” Dec. 01, 2024, *BioMed Central Ltd*.

[9] S. S. Chugh *et al.*, “The 2020 ESC Guidelines on the Diagnosis and Management of Atrial Fibrillation,” *Circulation*, vol. 129, no. 8, pp. 837–847, Feb. 2020.

[10] A. Kumar *et al.*, “Sudden cardiac death: Epidemiology, pathogenesis and management,” Mar. 01, 2021, *IMR Press Limited*.

[11] D. Koppad, “Arrhythmia Classification Using Deep Learning: A Review,” *WSEAS Transactions on*

Corresponding author: Annisa Humairani, annisahumairani@telkomuniversity.ac.id, School of Electrical Engineering, Telkom University, Bandung, Jl. Telekomunikasi No. 1, Sukapura, Kecamatan Dayeuhkolot, Kab. Bandung, Jawa Barat 40257.
DOI: https://doi.org/10.35882/jteknokes.v19i1.154

Biology and Biomedicine, vol. 18, pp. 96–105, Aug. 2021.

[12] H. Li and P. Boulanger, "An Automatic Method to Reduce Baseline Wander and Motion Artifacts on Ambulatory Electrocardiogram Signals," *Sensors*, vol. 21, no. 24, 2021.

[13] S. Elouaham, A. Dliou, W. Jenkal, M. Louzazni, H. Zougagh, and S. Dlimi, "Empirical Wavelet Transform Based ECG Signal Filtering Method," *Journal of Electrical and Computer Engineering*, vol. 2024, 2024.

[14] S. Suresh Kumar, K. Dashtipour, Q. H. Abbasi, M. A. Imran, and W. Ahmad, "A Review on Wearable and Contactless Sensing for COVID-19 With Policy Challenges," 2021, *Frontiers Media S.A.*

[15] M. F. Issa *et al.*, "Enhancing single-lead electrocardiogram arrhythmia detection with empirical mode decomposition," *Neural Comput Appl*, Jun. 2025.

[16] V. Gupta, M. Mittal, and V. Mittal, "Chaos Theory: An Emerging Tool for Arrhythmia Detection," *Sens Imaging*, vol. 21, no. 1, Dec. 2020.

[17] X. Bian, M. Ling, Y. Chu, P. Liu, and X. Tan, "Spectral denoising based on Hilbert–Huang transform combined with F-test," *Front Chem*, vol. 10, Aug. 2022.

[18] G. B. Moody and R. G. Mark, "MIT-BIH Arrhythmia Database," PhysioNet.

[19] H. Zakaria, E. S. H. Nurdiniyah, A. M. Kurniawati, D. Naufal, and N. Sutisna, "Morphological Arrhythmia Classification Based on Inter-Patient and Two Leads ECG Using Machine Learning," *IEEE Transactions on Automation Science and Engineering*, vol. 12, pp. 147372–147386, 2024.

[20] A. Sadoughi, M. B. Shamsollahi, and E. Fatemizadeh, "The Classification of Heartbeats from Two-Channel ECG Signals Using Layered Hidden Markov Model," *Frontiers in Biomedical Technologies*, vol. 9, no. 1, pp. 59–67, 2022.

[21] A. R. Vazifeh and J. W. Fleischer, "Manifold Learning for Personalized and Label-Free Detection of Cardiac Arrhythmias," Jun. 2025.

[22] C. Yang, E. A. Fridgeirsson, J. A. Kors, J. M. Reps, and P. R. Rijnbeek, "Impact of random oversampling and random undersampling on the performance of prediction models developed using observational health data," *J Big Data*, vol. 11, no. 1, Dec. 2024.

[23] P. Madona, R. I. Basti, and M. M. Zain, "PQRST wave detection on ECG signals," *Gac Sanit*, vol. 35, pp. S364–S369, Jan. 2021.

[24] S. Lamba, S. Kumar, and M. Diwakar, "FADLEC: feature extraction and arrhythmia classification using deep learning from electrocardiograph signals," *Discover Artificial Intelligence*, vol. 5, no. 1, Dec. 2025.

[25] A. Daffa Fakhrudin and P. Harry Gunawan, "Arrhythmia Classification Using CNN-SVM from ECG Spectrogram Representation," *Eduvest-Journal of Universal Studies*, vol. 4, no. 12, pp. 11245–11254, 2024.

[26] H. Ruan, X. Dai, S. Chen, and X. Qiu, "Arrhythmia Classification and Diagnosis Based on ECG Signal: A Multi-Domain Collaborative Analysis and Decision Approach," *Electronics (Switzerland)*, vol. 11, no. 19, Oct. 2022.

[27] S. Dalal and V. P. Vishwakarma, "Classification of ECG signals using multi-cumulants based evolutionary hybrid classifier," *Sci Rep*, vol. 11, no. 1, Dec. 2021.

[28] I. Enesi, M. Harizaj, and B. Cico, "Implementing Fusion Technique Using Biorthogonal Dwt to Increase the Number of Minutiae in Fingerprint Images," *J Sens*, vol. 2022, 2022.

[29] S. A. Malik, S. A. Parah, H. Aljuaid, and B. A. Malik, "An Iterative Filtering Based ECG Denoising Using Lifting Wavelet Transform Technique," *Electronics (Basel)*, vol. 12, no. 2, 2023.

[30] W. Chen *et al.*, "Hybrid DWT NLM method with NOA optimization for ECG signal denoising," *Sci Rep*, vol. 15, no. 1, Dec. 2025.

[31] C.-C. Lin, P.-C. Chang, and P.-H. Tsai, "A Dual-Adaptive Approach Based on Discrete Cosine Transform for Removal of ECG Baseline Wander," *Applied Sciences*, vol. 12, no. 17, 2022.

[32] MathWorks, "Dual-Tree Complex Wavelet Transforms," MathWorks Documentation.

[33] Q. Xie, S. Tu, G. Wang, Y. Lian, and L. Xu, "Discrete Biorthogonal Wavelet Transform Based Convolutional Neural Network for Atrial Fibrillation Diagnosis from Electrocardiogram," in *Proceedings of the Twenty-Ninth International Joint Conference on Artificial Intelligence, IJCAI-20*, C. Bessiere, Ed., International Joint Conferences on Artificial Intelligence Organization, Aug. 2020, pp. 4403–4409.

[34] R. Guido, S. Ferrisi, D. Lofaro, and D. Conforti, "An Overview on the Advancements of Support Vector Machine Models in Healthcare Applications: A Review," *Information*, vol. 15, no. 4, 2024.

[35] D. Donick and S. C. Lera, "Uncovering feature interdependencies in high-noise environments with stepwise lookahead decision forests," *Sci Rep*, vol. 11, no. 1, p. 9238, 2021.

[36] Z. Sun, J. Zhang, X. Zhu, and D. Xu, "How Far Have We Progressed in the Sampling Methods for Imbalanced Data Classification? An Empirical Study," *Electronics (Basel)*, vol. 12, no. 20, 2023.

[37] M. Sinnoor and S. K. Janardhan, "An Improved Firefly Optimization Algorithm for Analysis of Arrhythmia Types," *International Journal on Recent and Innovation Trends in Computing and*

Corresponding author: Annisa Humairani, annisahumairani@telkomuniversity.ac.id, School of Electrical Engineering, Telkom University, Bandung, Jl. Telekomunikasi No. 1, Sukapura, Kecamatan Dayeuhkolot, Kab. Bandung, Jawa Barat 40257.
DOI: https://doi.org/10.35882/jteknokes.v19i1.154

Communication, vol. 11, no. 7 S, pp. 430–436, Jul. 2023.

[38] H. Zakaria, E. S. H. Nurdiniyah, A. M. Kurniawati, D. Naufal, and N. Sutisna, "Morphological Arrhythmia Classification Based on Inter-patient and Two Leads ECG using Machine Learning," *IEEE Access*, 2024.

[39] C. Liang, M. K. M. Ali, and L. Wu, "A novel multi-class classification method for arrhythmias using Hankel dynamic mode decomposition and long short-term memory networks," *Journal of the Nigerian Society of Physical Sciences*, vol. 7, no. 2, May 2025.

[40] X. Zhao Hang AND Yin, "Deep VMD-attention network for arrhythmia signal classification based on Hodgkin-Huxley model and multi-objective crayfish optimization algorithm," *PLoS One*, vol. 20, no. 5, pp. 1–30, Aug. 2025.

[41] K. Dragomiretskiy and D. Zosso, "Variational Mode Decomposition," *IEEE Trans. Signal Process.*, vol. 62, no. 3, pp. 531–544, Feb. 2014.

[42] C. Torrence and G. P. Compo, "A Practical Guide to Wavelet Analysis," *Bull. Amer. Meteor. Soc.*, vol. 79, no. 1, pp. 61–78, Jan. 1998.

[43] D. Koppad, "Arrhythmia Classification Using Deep Learning: A Review," *WSEAS Trans. Biol. Biomed.*, vol. 18, pp. 96–105, Aug. 2021.

AUTHOR BIOGRAPHY

Amalia Nurul Maulida received the B.Eng. degree in Biomedical Engineering from Telkom University, Bandung, Indonesia, in 2025, graduating *summa cum laude* with a GPA of 3.91/4.00. During her undergraduate studies, she developed strong expertise in biomedical signal processing, machine learning, and data-driven healthcare systems. She previously joined the National Research and Innovation Agency (BRIN) as a Data Research Analyst, where she worked on gait data acquisition and analysis for neurological disorder studies, including integrating IMU sensors and electromyography (EMG) systems. Her interest in quantitative biomedical research led her to explore medical image analysis, particularly bone mineral density estimation using X-ray imaging, for which she received the Best Paper award at the International Conference on Information and Communication Technology (ICoICT) 2025. She is currently with PT PLN (Persero) as a Data Scientist, focusing on data transformation pipelines, dashboard development, sentiment analysis, and predictive maintenance analytics for industrial systems. Her research interests include biomedical signal and image processing, statistical learning, deep learning, and data science applications for both healthcare and energy sectors.

Annisa Humairani received the B.Eng. degree in Telecommunication Engineering from Telkom University, Indonesia, in 2020. She later obtained the M.Eng. degree in Telecommunication Engineering from the same university in 2022. She is currently a Lecturer in the Biomedical Engineering Study Program, School of Electrical Engineering, Telkom University Main Campus, Bandung, Indonesia, where she teaches and conducts research on AI and biomedical signal processing. She previously worked as a Product Solutions Engineer at ZTE Indonesia. Her research interests include biomedical signal processing, artificial intelligence, machine learning, and intelligent healthcare systems, with recent publications on EEG analysis, seizure detection, and early detection of Alzheimer's dementia.

Tito Waluyo Purboyo received his bachelor's degree in physics from Institut Teknologi Bandung, Indonesia, in 1998, and in Civil Engineering from Gadjah Mada University, Indonesia, in 2001. He earned his master's degree in mathematics from Institut Teknologi Bandung in 2009 and completed his doctoral degree in Electrical Engineering and Informatics from the same institution in 2015. He is currently a lecturer at Telkom University in Indonesia. His research interests include artificial intelligence, machine learning, network security, signal and system analysis, and mathematical modeling. His current work involves AI-aided ECG analysis, multi-lead wearable ECG, biomedical modelling, and biomedical device technology.

Dziban Naufal received the bachelor's degree in physics from Universitas Padjadjaran, Indonesia, in 2018, with a concentration in instrumentation and electronics, and the master's and Ph.D. degrees in biomedical engineering from the School of Electrical Engineering and Informatics, Institut Teknologi Bandung, in 2020 and 2023, respectively. His doctoral thesis focused on diagnosing heart failure through the analysis of heart vibrations and sound recordings. In 2024, he joined the Biomedical Engineering Department at the School of Electrical Engineering, Telkom University, as a Lecturer. His research interests include signal processing, instrumentation and control, system analysis, data mining, and physical modeling. His current works involve AI-aided ECG analysis, vascular biomechanics, and diagnostic technologies in hematology.

Corresponding author: Annisa Humairani, annisahumairani@telkomuniversity.ac.id, School of Electrical Engineering, Telkom University, Bandung, Jl. Telekomunikasi No. 1, Sukapura, Kecamatan Dayeuhkolot, Kab. Bandung, Jawa Barat 40257.
DOI: https://doi.org/10.35882/jteknokes.v19i1.154